Mechanism of Charge Transport in Anisotropic Layers of a Phthalocyanine Polymer

P. Gattinger,[†] H. Rengel,[‡] and D. Neher*[,§]

Max-Planck Institut für Polymerforschung, Ackermannweg 10, D-55128 Mainz, Germany

M. Gurka and M. Buck

Lehrstuhl für Angewandte Physikalische Chemie, University of Heidelberg, Im Neuenheimer Feld 253, D-69120 Heidelberg, Germany

A. M. van de Craats and J. M. Warman

Radiation Chemistry Department, IRI, Delft University of Technology, Mekelweg 15, 2629 JB Delft, The Netherlands

Received: September 16, 1998; In Final Form: January 25, 1999

Solid samples of phthalocyaninato-polysiloxanes (PcPS) have been analyzed by electrical dark conductivity experiments and by pulse-radiolysis time-resolved microwave conductivity (PR-TRMC) measurements. The in-plane conductivity of anisotropic PcPS Langmuir−Blodgett assemblies on gold surface-comb electrodes reveals an ohmic dependence at low voltages followed by a space-charge-limited current regime at higher electric fields. The conductivity displays a close to Arrhenius-type temperature dependence, with activation energies of 0.33−0.36 eV. The analysis of the space-charge limited currents (SCLC) experiments yields charge carrier mobilities of approximately $10^{-7}-10^{-6}$ cm^2/V^{-1} s^{-1} at room temperature. The conductivity perpendicular to the polymer chains was investigated by performing dielectric experiments on sandwich devices. These measurements reveal conductivities which are lower by several orders of magnitude than the corresponding in-plane values but the activation energy agrees quite well with that of the ohmic currents in the in-plane conductivity experiments. This result indicates that the same processes such as the hopping of charges in an energetically disordered material are involved in the transport. The intrachain mobility, as determined by PR-TRMC, is temperature-independent with a value of ca. 2×10^{-2} cm^2/Vs. The lack of any pronounced temperature dependence of the PR-TRMC mobility supports our conclusion that the electrical conductivities in the dc-surface-comb and ac-dielectric spectroscopy experiments are limited by temporary trapping or hindrance of motion of the charge carriers on particular sites during their transport over macroscopic distances.

Introduction

Phthalocyaninato-polysiloxanes (PcPS) (Figure 1) consist of phthalocyanine (Pc) rings which are covalently connected in a cofacial geometry.[1−3] A particularly interesting feature of these materials is the arrangement of the monomer units. At a repeat distance of 0.33 nm, the strong steric interaction between the disk-shaped repeat units forces the polysiloxane backbone to become rigid. This close cofacial arrangement also induces an electromagnetic coupling of the chromophore units. In the polymer the Q-band is considerably broadened and blue-shifted to 540−560 nm while the monomer exhibits the Q-band at 680 nm. These spectral changes can be explained by the theory of molecular excitons as given by Kasha.[4,5]

On peripheral alkoxy chain substitution, the polymers are soluble and can be processed by the Langmuir−Blodgett (LB) technique into thin films.[1,6,7] Details of the film architecture have been analyzed by combining X-ray diffraction,[8] and IR[9] and UV−vis spectroscopies.[3] The backbone of the hairy rod molecules is oriented parallel to the substrate surface. Consecutive transfer of monolayers leads to PcPS LB films with a layered structure and a monolayer thickness of approximately 2.2 nm. While the structure in as-prepared PcPS films is far

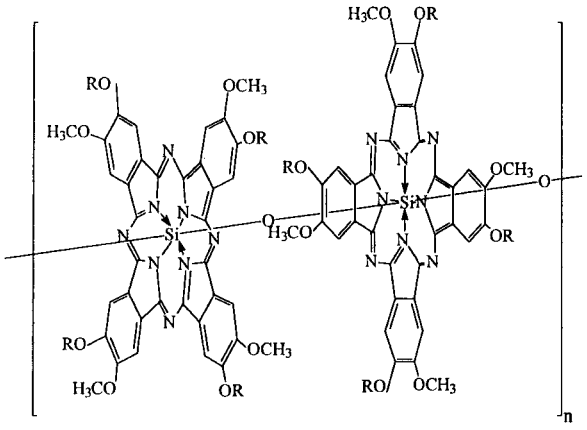

Figure 1. The molecular structure of the phthalocyaninato-polysiloxane polymers, PcPS, with R = C_8C_{17} and R = $C_{18}H_{37}$, denoted "C1C8" and "C1C18" in the text.

[†] Present address: Siemens AG, Wernerstr. 2, D-93049 Regensburg, Germany.

[‡] Present address: Boehringer Ingelheim Pharma KG, Binger Str. 173, 55216 Ingelheim, Germany.

[§] Present address: University of Potsdam, Institute for Physics, Am Neuen Palais 10, 14469 Potsdam, Germany.

10.1021/jp983734v CCC: $18.00
Published on Web 04/01/1999

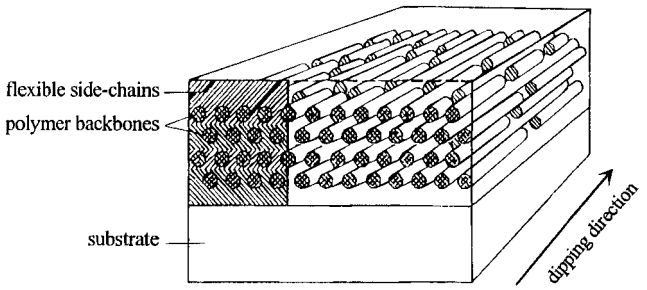

Figure 2. The structure of PcPS−Langmuir−Blodgett (LB) films with hexagonal packing of the PcPS rods.

from ideal, annealing leads to a highly oriented hexagonal packing of the cylinders.[8] The closest packed planes lie flat on the substrate surface, and the in-plane anisotropy is further improved as has also been seen in LB films based on other rigid rod polymers.[10,11] In those annealed layers the structure is that of an oriented hexagonal packing of cylinders of cofacially stacked conjugated macrocycles in a disordered matrix of aliphatic side chains (Figure 2). Transmission electron microscopy (TEM) measurements have shown that PcPS LB films consist of microdomains with dimensions of several tens of nanometers and a strictly parallel alignment of the molecules. For longer length scales disclinations are observed.[12] The flow conditions on the Langmuir trough generate a preferential alignment of the long axis of the PcPS molecules along the dipping direction.[13] This structural order is responsible for the pronounced anisotropy of various properties of these films.[9,14−19]

Due to its excellent thermal and particularly good electrochemical stability[20] PcPS has been examined with respect to electrical and photoelectrical properties.[14,17,19,21,22] In contrast to films of monomeric Pc, where different polymorphic structures can be present depending on the method of preparation and temperature, the covalent link in PcPS forces the macrocycles into a strict cofacial stacking. While rotational motion of the rings is possible even in the solid state as confirmed by solid-state NMR spectroscopy,[23] a significant deviation of the rings from the cofacial arrangement is quite difficult. Even though there is no orbital overlap between the Pc macrocycles it is expected that electron motion within the core of the stack will be rapid compared to the motion perpendicular to the polymer backbone which would involve tunneling through the aliphatic side chains. This makes PcPS a model system for the study of charge transport in materials with an intrinsically one-dimensional conductivity. The layer-wise deposition of the PcPS molecules enables the control of the molecular orientation within the films. The degree of in-plane anisotropy can be measured by optical spectroscopy. This makes these materials particularly suitable for the analysis of charge transport processes compared to most semiconducting polymers which can only be processed by casting or spin coating from solution.

This contribution summarizes experiments on the anisotropy of the electrical dark conductivity in LB assemblies of PcPS as well as results from pulse-radiolysis time-resolved microwave conductivity measurements (PR-TRMC) on isotropic samples. The conductivity was studied as a function of the electric field and temperature in all three directions. The in-plane conductivity was measured using PcPS−Langmuir−Blodgett assemblies on gold surface-comb electrodes with the field applied parallel and perpendicular to the dipping direction. In both cases the macroscopic conductivity involves charge transport parallel and perpendicular to the polymer backbones as the in-plane orientational distribution is rather broad. Sandwich-type devices where used to analyze the charge carrier motion strictly perpendicular to the polymer backbones.

Experimental Section

The synthesis of PcPS has been described elsewhere.[1,2] Two types of PcPS polymers, tetra(methoxy)-tetra(octyloxy)-PcPS (C1C8) and tetra(methoxy)-tetra(octadecyloxy)-PcPS (C1C18) were studied. While both polymers can be processed with the LB technique, only films of C1C8 give rise to a pronounced in-plane anisotropy of orientation. All dark-conductivity experiments have been performed on Langmuir−Blodgett assemblies of C1C8. On the basis of neutron scattering experiments on a C1C8 compound with similar solubility and optical properties to the present material, the molecular weight M_w of the compound used can be estimated to be 38.000 g/mol, corresponding to 32 repeat units or a length of approximately 10 nm.[19,24]

Films were prepared by spreading a dilute solution of PcPS in chloroform onto the water surface of a Lauda-LB trough. Subsequently, the compressed PcPS LB monolayers were transferred onto the patterned substrates (see below) by vertical dipping at a surface pressure of 25 mN/m ($T = 18$ °C) and a relatively high dipping speed of 23 mm/min. Before performing the experiments, the samples were subject to annealing, typically at a temperature of 100 °C for several hours, to improve the structural quality of the films.

For the measurements of the in-plane conductivities of PcPS films a defined number of layers were deposited on fused silica substrates (25×12.5 mm^2), patterned with interdigitating gold electrodes. The thickness of the gold was either 40 or 50 nm and a 5 nm (10 nm) interlayer of chromium served as adhesion promotor. The electrodes covered an area of about 5×5 mm^2. The interdigitated electrode strips were 30 or 10 μm apart, and the total electrode length (given by the number times length of the strips) was 0.42 and 1 m, respectively. Each sample had two sets of electrodes arranged orthogonally to each other. Thus current voltage (I/U-) curves with the electric field parallel and perpendicular to the dipping direction could be recorded on the same sample. Recent AFM investigations of an LB monolayer on a 15 nm high surface electrode structure has demonstrated that the electrodes do not disturb the alignment and order of the PcPS molecules in the layer.[25]

Charge transport perpendicular to the LB monolayers has been investigated in Au/PcPS/Al sandwich structures with 80 monolayers of PcPS. Quartz substrates for LB deposition were hydrophobized with dimethyl-dichlorosilane in order to improve the transfer of PcPS onto the substrate. This was followed by thermal evaporation of the semitransparent bottom electrode (chromium 3 nm + gold 22 nm), onto which the PcPS LB monolayers were transferred. The films were subsequently annealed in air for more than 12 h at a temperature of 110 °C. Next, the aluminum top electrode was thermally evaporated in a vacuum (10^{-5} mbar) at an average rate of 0.07 nm/s using a pulse technique.[26] Pulsing reduces the risk of thermal damage and sample short circuits. A thickness of 26 nm was chosen to form a well-conducting electrode. The active area defined by the intersection of the top and bottom electrode strips, measured approximately 2×2 mm.[2] Currents were measured using an electrometer (Keithley 617), and an IBM personal computer was used for data acquisition and control of parameters.

Using PR-TRMC, a very low concentration (about 10 μM) of electron−hole pairs is produced uniformly throughout the material by a short pulse of ionizing radiation. This procedure, referred to as "radiation doping", does not perturb the primary

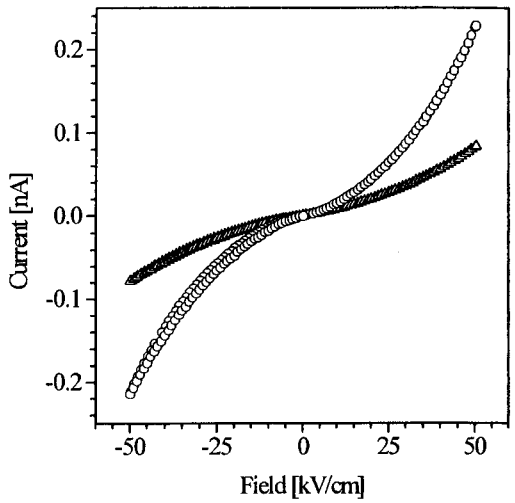

Figure 3. *I*/*U* characteristics of a film of 31 LB layers of C1C8 on interdigitated electrodes recorded at room temperature. The electrode distance is 10 μm. Measurements started at 0 V in the "positive" direction. The electric field was either parallel (circles) or perpendicular (triangles) to the dipping direction.

molecular or higher order structure of the material. If the charge carriers are mobile, an increase in conductivity will occur which is monitored with nanosecond time resolution as a decrease in the power level of microwaves which traverse the sample. Since the concentration of charge carrier pairs formed can be estimated, the mobility $\Sigma\mu$ can be determined. Because of the ultrashort time scale of the measurements charge carriers are usually observed before they recombine or have time to become localized at chemical (e.g., O_2) or physical (e.g., grain boundary) defects. The mobilities determined can, therefore, be considered to be "trap free". The use of 30 GHz microwaves to probe the conductivity change has the advantage over dc techniques that complications due to electrode contacts, space-charge, and domain or grain boundaries are absent. Effects due to structural disorder should also be minimized. As a result, the mobilities derived refer to the maximum value that could possibly be obtained in a dc-drift experiment with a perfectly orthogonally oriented monodomain of a columnar discotic material between the electrodes. Good agreement has in fact been found between charge carrier mobilities determined using dc time-of-flight (TOF) and PR-TRMC methods for the liquid crystalline phases of the columnar discotic material hexa-hexylthio-triphenylene.[27] Full details of the experimental technique and data analysis have been published elsewhere.[28,29]

Results

In-Plane Conductivity. Figure 3 displays current voltage (*I*/*U*) characteristics of an annealed PcPS film of 31 LB layers measured in a high vacuum environment (10^{-8} mbar range) at room temperature parallel (p) and perpendicular (s) to the dipping direction. Since the current did not immediately follow the change of the voltage but showed a retarded response, it was measured after a 30 s equilibration time at each voltage step. Complete cycles over $\pm$50 V were measured starting at 0 V. Typically, the curves exhibited a slight hysteresis, whose magnitude depended on the details of the experimental conditions, and possessed a small asymmetry with respect to the origin (Figure 3). This indicates that the *I*/*U* characteristics depend to some extent on the sample history, i.e., on the number of charge carriers trapped in the film. Furthermore, the dark conductivity at a given temperature and voltage varies significantly from

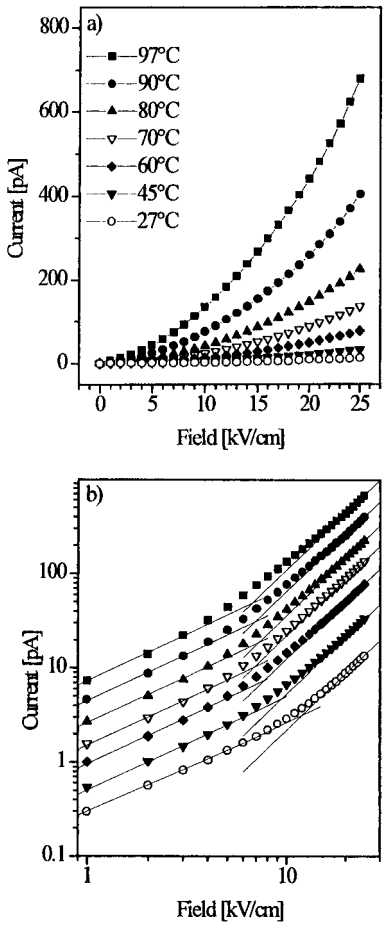

Figure 4. *I*/*U* characteristics of a film of 11 LB layers of C1C8 on interdigitated electrodes recorded at different temperatures. The electrode distance is 10 μm. The field was applied parallel to the dipping direction. (a) Linear representation, (b) double-logarithmic plot. The straight lines indicate the dependence expected for low-field ohmic and high-field SCLC conduction.

sample to sample. Typically, in-plane conductivities parallel to the dipping direction range between 10^{-9} and 10^{-10} S/cm. The conductivity anisotropy is about 3. Values for the in-plane conductivity anisotropy of PcPS LB films are, however, sample dependent and range between 2 and 10.[19] This variation is thought to be due to the effects of film microstructure including domain size and the degree of alignment of the PcPS molecules. A clear correlation between the optical anisotropy and the conductivity anisotropy has been demonstrated recently.[19]

Information on the charge carrier mobility was derived from experiments performed over a large voltage range. On the basis of the work function of gold and the oxidation and reduction potentials of PcPS, we can conclude that Au forms an ohmic contact for holes. The current density is, therefore, not expected to be injection limited[14] and, depending on the voltage, either an ohmic or space-charge-limited current (SCLC) should be observed. At low fields the current density j is described by Ohm's law

$$j_\Omega = ne\mu\frac{U}{d} \tag{1}$$

whereas at higher fields Child's law for space charge limited current (SCLC) applies:

$$j_{SCLC} = \frac{9}{8}\epsilon_0\epsilon\mu\frac{U^2}{d^3} \tag{2}$$

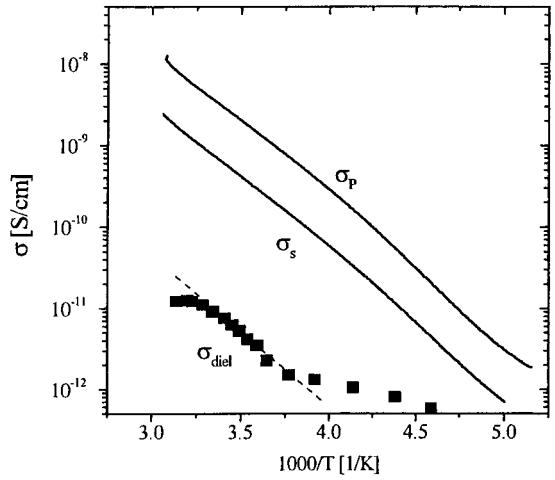

Figure 5. The temperature dependence of the conductivity of 11 LB layers of C1C8 on interdigitated electrodes (spacing 10 μm) at a fixed voltage of 10 V. σ_p and σ_s are the conductivities parallel and perpendicular to the dipping direction, respectively. The conductivity anisotropy is 5.4 independent of temperature. Solid squares show the ac conductivity with no external bias for a frequency of 20 Hz as measured on a Au/PcPS (80 layers)/Al sandwich structure. The dashed line corresponds to an activation energy of 0.36 eV.

Here, μ, d, and ϵ denote the mobility, the electrode separation, and the dielectric constant. n is the charge carrier density initially present in the material at low voltages, which is introduced by doping, impurities, or by thermal activation.

For some well-annealed samples the ohmic conductivity was low and a SCLC regime could be clearly resolved. The current−voltage characteristics of such a sample are displayed in Figure 4, which shows the results for a film of 11 LB layers at various temperatures. The measurements were performed by starting at 97 °C and decreasing the temperature stepwise to room temperature. As above, the measurements were performed under ultrahigh vacuum conditions. The curves represent the first part of a voltage cycle, i.e., the increase from 0 to 25 kV/cm. The double-logarithmic plot of Figure 4b reveals the transition from ohmic to space-charge-limited behavior. The straight lines represent the ohmic and space-charge-limited regime according to eq 1 and eq 2, respectively. The onset of the transition from the ohmic to the SCLC region shifts only slightly to lower fields with increasing temperature.

According to eq 2 the charge carrier mobility μ can be deduced from the current density in the SCLC regime. The data of Figure 4 yield a temperature dependence of the mobility with values ranging between 3.6×10^{-7} at 27 °C and 2.1×10^{-5} cm^2/Vs at 97 °C. Knowing μ, the initial density of charge carriers n can be calculated from the ohmic part of the curve according to eq 1. For the set of data shown in Figure 4 values for n are approximately 1×10^{13} cm^{-3} (1.9×10^{13} cm^{-3} at 27 °C, 8.9×10^{12} cm^{-3} at 97 °C). In contrast to the increase in mobility by 2 orders of magnitude upon raising the temperature, the carrier density n in the ohmic region remains almost constant.

Figure 5 shows the conductivity in the ohmic regime parallel and perpendicular to the dipping direction as a function of temperature for an annealed film in nitrogen atmosphere. Over several decades in current the conductivity follows an Arrhenius-type activation behavior. Since the anisotropy remains constant throughout the whole temperature range, both σ_p and σ_s must exhibit similar activation energies of approximately 0.33 eV.

Charge Transport Perpendicular to the Molecular Orientation. Charge transport in PcPS films perpendicular to the substrate surface has been investigated in Au/PcPS/Al sandwich

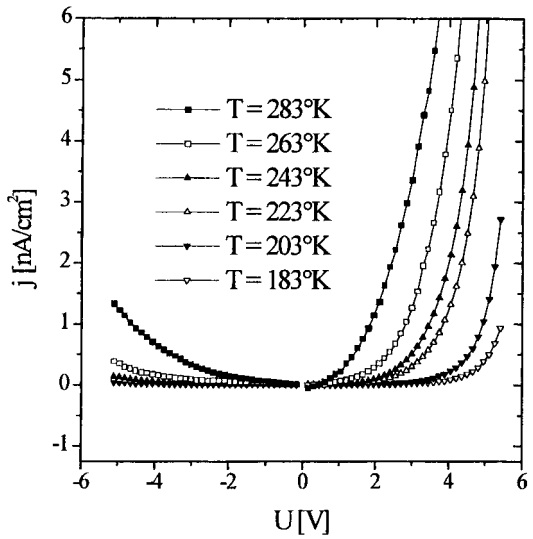

Figure 6. Current density versus applied external bias for an Au/C1C8 (80 layers)/Al sandwich structure measured at different temperatures. Positive voltages refer to the Au electrode biased as the anode.

structures of 80 LB layers. These devices show a pronounced rectifying behavior (Figure 6). The energy levels determined by cyclic voltammetry indicate a charge injection barrier of approximately 1 eV for holes from Al into the PcPS layer. In agreement with this, the reverse current can be modeled by the thermionic injection of holes from the aluminum electrode into the PcPS film.[14] Further, photovoltaic experiments have indicated the existence of a space-charge region at this interface.[14] The *I*/*V* characteristics for forward bias can neither be described by a pure Schottky-diode behavior nor by the Fowler−Nordheimer equation for tunnel injection. We conclude that the dc current is affected by the bulk conductivity perpendicular to the rods, too. Unfortunately, we did not succeed in evaporating metals with a larger work function, such as Ag or Au, as top electrode materials without causing electrical shorts through the sample.

To separate interface from bulk effects, dielectric spectroscopy was performed. Figure 7 shows the AC conductivity and the capacitance of a sandwich device with no additional bias applied. In the frequency regime between 1 and 100 Hz a plateau region of the conductivity is observed. The measured conductivity is temperature dependent and the capacitance corresponds to the geometric capacitance. The conductivity in this regime reflects the bulk charge transport perpendicular to the polymer backbone. At lower frequencies an increase of the capacitance and a decrease of the conductivity is observed. This effect is caused by a polarization of the device which is due either to the accumulation of charges at the metal−PcPS interface or to a change in the width of the space charge layer close to the Al electrode. At frequencies above 1000 Hz the conductivity rises again while the capacitance remains constant. This additional process is caused by the resistance of the thin, vacuum evaporated, electrodes in conjunction with the capacitance of the sample. If an additional dc bias of up to −3 V is applied in the reverse direction, the conductivity in the plateau region changes only slightly even though the dc current through the device increases by approximately 1 order of magnitude in the same voltage range. This proves that a certain density of mobile charge carriers must initially be present in the PcPS bulk, which is larger than the number of charge carriers injected at reverse bias. At forward bias the current both at low frequencies and in the plateau region increases and finally become similar in magnitude. At this point the charge carrier density should be

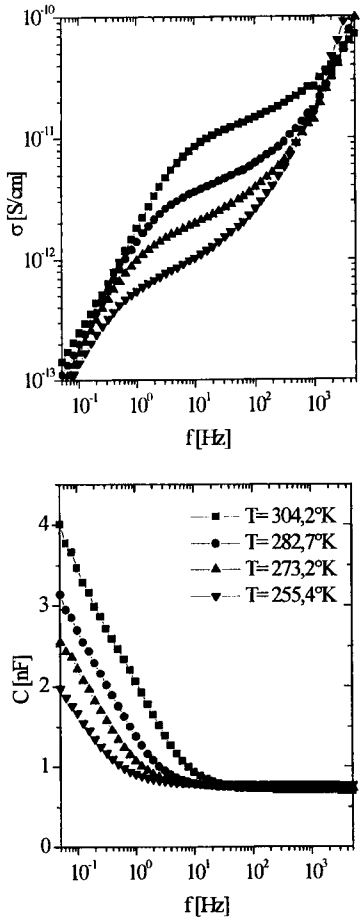

Figure 7. The ac conductivity and capacity of an 80 LB layer C1C8 sample between Au and Al as determined from the real and imaginary part of the dielectric function in the dielectric experiments.

determined by the injection of charges. The behavior at high frequencies is independent of bias, indicating that the effect is not related to the properties of the PcPS film but depends solely on the device geometry and the presence of external resistors.

A comparison of the charge transport parallel and perpendicular to the PcPS rods must be based on experiments, which reflect the intrinsic transport properties of the PcPS film. In the ohmic regime of the surface comb electrical measurements and in the plateau region of the dielectric experiments at no or reverse bias, the conductivity is proportional to the charge carrier mobility and the initial density of charge carriers. The latter can be assumed to be similar in magnitude for both sets of samples. ac conductivities as derived from the dielectric experiments with no external bias on a Au/PcPS/Al sandwich structure (σ_{diel}) are compared with data measured in the ohmic regime in the surface-comb geometry in Figure 5. Within the temperature range exhibiting a plateau in the ac-frequency dependence, as shown in Figure 7, σ_{diel} is Arrhenius-type activated with an activation energy of 0.36 eV. This value is similar to those derived from the conductivity data in the surface-comb geometry. At the same temperature the absolute conductivities perpendicular to the rods are, however, smaller by 2−3 orders of magnitude than the in-plane conductivities. Since the macroscopic charge transport perpendicular to the hairy rod orientation involves tunneling through aliphatic side chain regions, it is not surprising that the effective mobility in this direction is also orders of magnitude lower compared to the in-plane mobility. The presence of the barrier at the aluminum/PcPS interface, unfortunately, prevents the determination of the absolute mobility from the analysis of the DC current−voltage characteristics at higher fields.

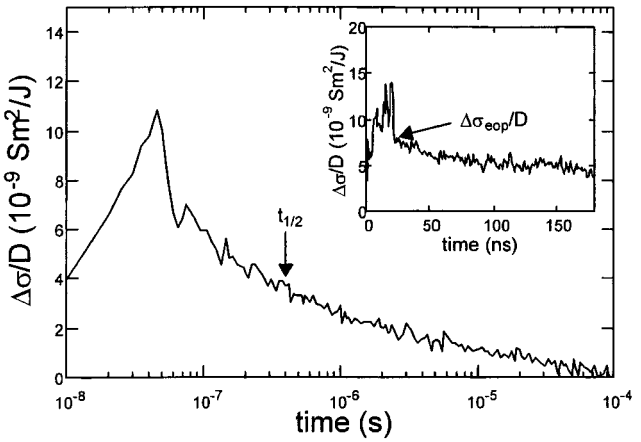

Figure 8. Main figure: The transient change in the conductivity of the C1C18 polymer on pulse-radiolysis (20 ns pulse) at room-temperature monitored using a logarithmic time scale with a 20 ns pulse and a time-response of 10 ns. The first half-life of the conductivity $t_{1/2}$ is indicated by the vertical arrow. Inset: The same transient taken on a linear time scale which was used to determine the end-of-pulse conductivity per unit dose $\Delta\sigma_{eop}/D$ as indicated by the arrow.

PR-TRMC. Figure 8 shows the PR-TRMC transients for the C1C18 derivative with, in the main Figure, data taken on a logarithmic time scale from 10^{-8} to 10^{-4} s, and in the inset data taken on a linear time scale over the first 180 ns. From the latter the end-of-pulse conductivity per unit dose (D J/m^3), $\Delta\sigma_{eop}$/D, is determined as illustrated. The one-dimensional, intracolumnar mobility $\Sigma\mu_{1D}$ can be derived from this experimental parameter using the following relationship,[27]

$$\sum\mu_{1D} = 3E_p(\Delta\sigma_{eop}/D)/F_{eop} \quad (3)$$

The values of the pair formation energy $E_p = 25$ eV and the end-of-pulse pair survival probability $F_{eop} = 0.35$ (C1C8) and 0.46 (C1C18), were estimated as described previously[30] and used to calculate the values of $\Sigma\mu_{1D}$ given in Figure 9A. As can be seen, $\Sigma\mu_{1D}$ is almost independent of temperature from 0 to 120 °C. In addition, similar values are found for both the C1C8 and C1C18 compounds. This supports the assumption that the mobility does indeed refer to intracolumnar charge transport, i.e., it is independent of the average distance between the columns L which varies from 22 to 37 Å. The average value of $\Sigma\mu_{1D}$, given by the horizontal straight line in Figure 9a, is 0.018 cm^2/Vs.

In previous TRMC measurements[28,31] on a C9C9 polysiloxane derivative the mobility was also found to display only a small temperature dependence. The absolute value, however, was a factor of 3 larger than the average value for the present compounds. This can be explained by an additional degree of disorder in the C1C8 and C1C18 compounds resulting from the random nature of substitution of the two different alkoxy side chains.

For comparison, mobility data previously published[30] for the monomeric, uniformly substituted C9C9 compound are displayed in Figure 9a. These are significantly larger than for the polymeric compounds over the entire temperature range and clearly display the sharp decrease at the crystalline solid to liquid crystal transition which has been found to be characteristic of the *n*-alkyl, substituted monomeric compounds. The decrease is attributed to the increase in intracolumnar disorder when the alkyl chains "melt" which has a negative influence on the charge

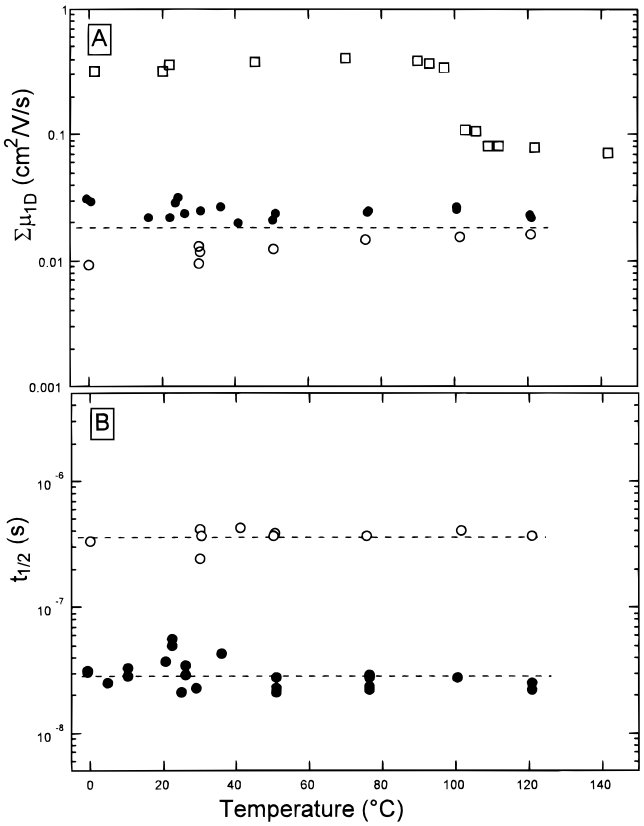

Figure 9. (a) The temperature dependence of the one-dimensional, intracolumnar mobility calculated from $\Delta\sigma_{eop}/D$ for C1C8 (filled circles) and C1C18 (open circles). Data for the monomeric C9C9 compound (open squares) are included for comparison. (b) The temperature dependence of the first half-life of the conductivity transients for C1C8 and C1C18 using the same symbols as in (a).

carrier mobility. For the polysiloxane compounds no evidence of a transition to a crystalline phase has been found in DSC or polarization microscopy measurements in agreement with the lack of a sharp transition in the $\Sigma\mu_{1D}$ data of the present study.

The eventual after-pulse decay of the conductivity, an example of which is shown for C1C18 at room temperature in Figure 8, displays disperse kinetics. As in the past,[31] we take the first half-life time $t_{1/2}$ as indicated in Figure 8 to be a characteristic measure of the time scale for the decay. The values of $t_{1/2}$ determined are plotted against temperature in Figure 9b. In contrast to $\Sigma\mu_{1D}$, $t_{1/2}$ is seen to be very different for the two polymers with that for C1C18 approximately an order of magnitude larger than that for the shorter alkyl chain compound. This effect has previously been found for the monomeric compounds and is taken to indicate that the decay process involves charge recombination via intercolumnar electron tunneling through the intervening saturated hydrocarbon mantle.[31]

As for $\Sigma\mu_{1D}$, $t_{1/2}$ is seen to be almost independent of temperature with values of 30 and 380 ns given by the horizontal straight lines in Figure 9b for C1C8 and C1C18, respectively. This temperature independence of the rate of long-distance electron tunneling through saturated hydrocarbon barriers has also been found for charge recombination in model donor−bridge−acceptor molecules.[32] The absolute rates for a given distance have been found to be of the same order of magnitude for charge recombination as those for single charge tunneling, i.e., in the absence of a coulomb field.[33,34] Taking this to be the case for the present systems, we can derive at least an approximate estimate for the two-dimensional, intercolumnar diffusion coefficient of charge using the $t_{1/2}$ values as first

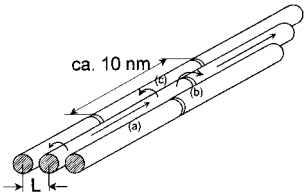

Figure 10. Schematic representation of charge transport within a domain of parallel oriented PcPS molecules.

approximations of the intercolumnar jump times, together with the known intercolumnar distances L,

$$D_{2D} = L^2/4t_{1/2} \tag{4}$$

From this, the Einstein relation between the diffusion coefficient and the low-field mobility, $D = \mu k_B T/e$, can be used to derive the mobility,

$$\mu_{2D} = eL^2/4k_B T t_{1/2} \tag{5}$$

The value of μ_{2D} found for room temperature using this approach and the values of $t_{1/2}$ and L given above are 1.6×10^{-5} cm^2/Vs and 0.4×10^{-5} cm^2/Vs for the C1C8 and C1C18 compounds, respectively. We emphasize that these values are only order-of-magnitude estimates. They do, however, indicate, by comparison with the value of ca. 0.02 cm^2/Vs for $\Sigma\mu_{1D}$, that the mobility perpendicular to the columnar axes should be approximately 3 orders of magnitude lower than for intracolumnar charge transport as was in fact found in the LB films measurements.

Discussion

TEM measurements on monomolecular layers of the present compounds have shown the existence of microdomains of several tens of nanometers in length and width with strictly parallel alignment of the molecules.[12,36] Within such a domain charge transport occurs by three processes: (a) transport along a single PcPS molecule, (b) hopping between successive molecules along the chain axis, or (c) intercolumnar hopping between adjacent molecular stacks (Figure 10). Depending on the direction of applied electric field one or more of the three contributions may dominate the conductivity. TEM micrographs did, however, not reveal the position of individual chain ends within a column. This indicates that the chain-to-chain separation between successive PcPS molecules in the same column is rather small and, therefore, process (b) might not present a significant limitation to charge carrier motion.

The PR-TRMC results show that at the microscopic level processes (a) and (b) are described by a temperature independent intracolumnar mobility of approximately 2×10^{-2} cm^2/Vs while the intercolumnar hopping occurs with a temperature-independent rate, which decreases with increasing lengths of the alkyl chains. On a macroscopic scale this intercolumnar motion strictly perpendicular to the polymer chains is expected to dominate the charge transport in the sandwich device. The ac-dielectric data, however, reveal a pronounced temperature dependence of the conductivity. One might conclude that the conductivity can be described by a temperature dependent charge carrier density and a constant mobility, with free charge carriers (holes) thermally generated through the ionization of neutral acceptor levels above the valence band at the observed activation energy. Since the activation energy for in-plane charge transport is the same as that perpendicular to the rods, μ_p and μ_s should also be independent of temperature. This is in clear contrast to the

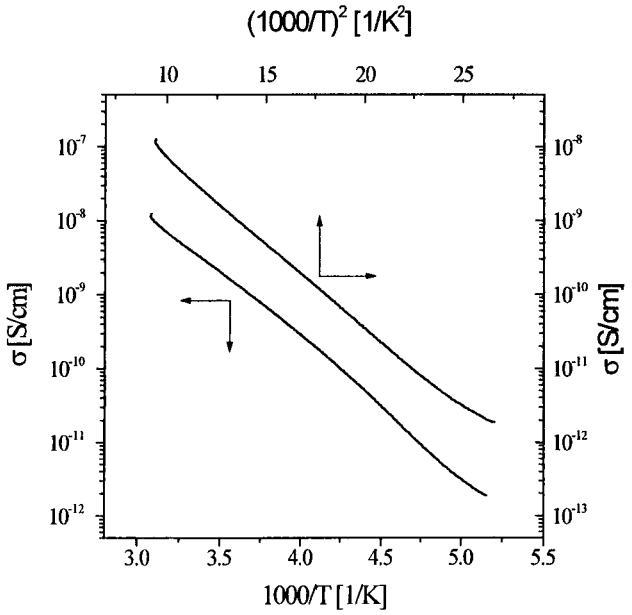

Figure 11. Representation of the temperature dependence of the in-plane conductivity σ_p from Figure 5 according to the Arrhenius and Bässler (eq 6) relation.

observations in the SCLC regime for in-plane conductivity as described above (Figure 4). We, therefore, conclude that the total density of charge carriers available in the material in the ohmic region is close to temperature independent and that the mobility increases with temperature.

The value of μ determined from the SCLC in the surface comb geometry increases from 10^{-7} to 10^{-5} cm^2/Vs with increasing temperature. To check the estimate of μ derived from the conductivity data in the SCLC regime we have determined μ at RT by introducing a controlled density of mobile holes (radical cations) into a PcPS film by electrochemical doping.[37] At low doping levels y the low field conductivity increased linearly with y. The analysis of the conductivity according to eq 1 (with n given by the doping level) yielded a hole mobility $\mu \cong 10^{-6}$ cm^2/Vs, which agrees with the value of μ as derived from the SCLC experiments at *RT*.

It has been shown that the temperature dependence of hole mobilities in thin films of monomeric phthalocyanines[38,39] and porphyrins prepared by vacuum sublimation[40] could be well described by the disorder formalism of Bässler and co-workers,[41] which predicts

$$\mu(T) = \mu_0 \exp\{-(2\kappa/3kT)^2\} \quad (6)$$

Here, κ is a parameter related to the energetic disorder and describes the width of the density of states distribution (DOS) of hopping sites. If the same data would be plotted in an Arrhenius fashion, the apparent activation energy E_a from the slope of log μ versus $1/T$ at a given temperature is

$$E_a = \frac{8\kappa^2}{9kT} \quad (7)$$

For the vacuum sublimed phthalocyanine films, the value of κ and thus the apparent activation energy in a small temperature window was a clear function of the sublimation rate and thus of the packing of the Pc rings. For the same compounds, κ ranged between 0.078 and 0.10 eV corresponding to apparent activation energies at RT of 0.22 and 0.36 eV, respectively. The value for the high-temperature preexponential mobility μ_o ranged between 2×10^{-3} and 5×10^{-3} cm^2/Vs, close to $\Sigma\mu_{1D}$ as determined here in the PR-TRMC experiments.

In molecular solids the broadening of the DOS originates from a variation in the orientation and distance between the charge-transport sites and the surrounding polar and nonpolar molecules. In PcPS the macrocycles are linked in a coplanar fashion which does not allow significant positional or orientational disorder. Within a domain, the PcPS cylinders are well ordered in parallel columns. Energetic disorder might, however, be introduced by the orientation of the dipoles in the alkoxy side chains or the nonsymmetric side chain substitution pattern. Also note that the side chain region is completely amorphous and that the individual Pc rings can rotate around the cylinder axis, introducing structural disorder. Evidence for considerable energetic disorder stems from the comparison of μ_{1D} for C1C8 and C1C18 with previously reported data[30] for the monomeric, uniformly substituted C9C9 compound as displayed in Figure 9a. If we take $E_a = 0.35$ eV as the apparent activation energy eq 7 gives a width κ of 0.1 eV with $T = 295$ K. Note that a decision on whether temperature-dependent mobility or conductivity data are better described by eq 6 or by an Arrhenius-type activation can only be made if data have been measured over a wide temperature range. For our experiments both models give reasonable fits as shown in Figure 11 for $\sigma_p(T)$, but the representation according to Bässler's model seems to be more meaningful at medium temperatures. Setting $\mu(RT) = 10^{-6}$ cm^2/Vs and $\kappa = 0.1$ eV, the limiting μ_o according to eq 6 is 10^{-3} cm^2/Vs, which is reasonable with respect to μ_{1D} of 10^{-2} cm^2/Vs. In contrast $\mu = \mu_o \exp(-E_a/kT)$ with $E_a = 0.35$ eV yields an unreasonably large limiting mobility of 1.2 cm^2/Vs. At this point we would like to emphasize that even though there is a clear preferential in-plane orientation parallel to the dipping direction, the orientational distribution function was shown to be broad[10,11] and both σ_p and σ_s involve both intra- and intercolumnar transport processes. Second, disclinations and domains with different orientations can be observed in the TEM micrographs and even σ_p requires jumps between adjacent columns in order to transport charges across macroscopic distances or to escape trapping within a disclination. Therefore, the macroscopic in-plane charge carrier mobility will always be smaller than μ_{1D}.

The temperature independence of the mobility derived from the PR-TRMC measurements arises from a combination of the short (nanosecond) time scale of the observations and the ultrahigh frequency of the electric field. Because of this it is the "trap-free" mobility that is in fact measured by PR-TRMC. In recent TOF and PR-TRMC studies of a deca-alkoxy substituted triphenylene dimer the intracolumnar mobility values were found to be closely similar for both techniques at elevated temperatures.[42] At lower temperatures, however, the TOF mobility was found to decrease dramatically while that determined by PR-TRMC remained almost constant, similar to the observations for the present compounds. The results were found to be consistent with a one-dimensional hopping model of charge transport with static energy disorder resulting from structural disorder within the columns. Both sets of mobility values could be reproduced by computer simulations of thermally activated jumps over barriers with an exponential distribution of the barrier heights (mean value 0.024 eV) and a jump frequency of 1 ps^{-1}. A similar explanation almost certainly underlies the different temperature dependences found for the mobilities determined for the present compounds using the dc or microwave methods of measurement.

Conclusion

The study of electric conductivity in different geometries and time scales reveals several mechanism which limit the charge carrier mobility and the conductivity in solid PcPS samples. The carrier mobility μ_{1D} prior to trapping as determined by PR-TRMC experiments is temperature independent with $\mu_{1D} \approx 2 \times 10^{-2}$ cm^2/Vs. The independence of μ_{1D} on the side chain length indicates that only transport parallel to the chain axis is involved. Mobilities over macroscopic distances of PcPS LB films parallel to the preferential chain orientation are approximately $10^{-7}-10^{-6}$ cm^2/Vs at room temperature.

Charge carrier transport perpendicular to the polymer chains involves tunneling through the aliphatic side chain regions. From PR-TRMC relaxation times a temperature-independent value of $\mu_{2D} = 10^{-5}$ cm^2/Vs is derived. This is 3 orders of magnitude smaller than the intracolumnar mobility μ_{1D} and proves that charge transport on a microscopic scale, for example, within a domain of highly oriented PcPS chains must be highly anisotropic. In agreement with this, the dark conductivity "strictly" perpendicular to the polymer backbones is smaller by approximately 3 orders of magnitude than the corresponding in-plane conductivity and it follows an Arrhenius-type temperature dependence with $E_a \approx 0.36$ eV. This value is similar to that of the temperature dependent in-plane conductivity.

It is, therefore, reasonable to assume that static or slow dynamic energetic disorder within the PcPS chains is mainly responsible for the difference between macroscopic dark conductivities and the PR-TRMC mobilities for transport parallel as well as perpendicular to the polymer backbone. Since a variation in site energy influences both the hopping parallel and perpendicular to the Pc chains, we expect the same apparent activation energies for the conductivities σ_p, σ_s, and σ_{diel}. This is observed experimentally. On the other hand, the rather good agreement between the microscopic mobility anisotropy μ_{1D}/μ_{2D} and the macroscopic conductivity anisotropy σ_p/σ_{diel} suggests that the anisotropy of the macroscopic charge transport is strongly related to the anisotropy of the microscopic transport processes.

Acknowledgment. We thank Prof. G. Wegner (MPI Mainz) and Prof. M. Grunze (University Heidelberg) for support and discussions. Financial support by the German Science Foundation (DFG) and the Volkswagen foundation is gratefully acknowledged.

References and Notes

(1) Sauer, Th.; Wegner, G. *Mol. Cryst. Liq. Cryst.* **1988**, *162*, 97.
(2) Caseri, W.; Sauer, T.; Wegner, G. *Makromol. Chem., Rapid Commun.* **1988**, *9*, 651.
(3) Sauer, T.; Caseri, W.; Wegner, G. *Mol. Cryst. Liq. Cryst.* **1990**, *183*, 387.
(4) Kasha, M.; Rawls, H. R.; Ashraf El-Bayouni, M. *Pure Appl. Chem.* **1965**, *11*, 371.
(5) Rae, E. G.; Kasha, M. In *Physical Processes in Radiation Biology*; Augenstein, L., Mason, R., Rosenberg, B. Eds.; Academic Press: New York, 1964
(6) Orthmann, E.; Wegner, G. *Angew. Chem.* **1986**, *98*, 1114.
(7) Orthmann, E.; Wegner, G. *Angew. Chem., Int. Ed. Engl.* **1986**, *25*, 1105.
(8) Albouy, P. A.; Schaub, M.; Wegner, G. *Acta Polymer* **1994**, *45*, 210.
(9) Sauer, Th.; Arndt, Th.; Batchelder, D. N.; Kalachev, A. A.; Wegner, G. *Thin Solid Films* **1990**, *187*, 357.
(10) Mittler-Neher, S.; Neher, D.; Stegeman, G. I.; Embs, F. W.; Wegner, G. *Chem. Phys.* **1992**, *161*, 289.
(11) Cha, M.; Neher, D.; Embs, F. W.; Mittler-Neher, S.; Stegeman, G. *Chem. Phys. Lett.* **1993**, *202*, 44.
(12) Wu, J.; Lieser, G.; Wegner, G. *Adv. Mater.* **1996**, *8*, 151.
(13) Wegner, G.; Mathauer, K. *Mater. Res. Soc.* **1992**, *274*, 767.
(14) Gattinger, P.; Rengel H.; Neher, D. *J. Appl. Phys.* **1998**, *84*, 3731.
(15) Bubeck, C.; Neher, D.; Kaltbeitzel, A.; Duda, G.; Arndt, T.; Sauer, T.; Wegner, G. In *Nonlinear Optics in Polymers*; Messier, J., Kajzar, F., Prasad, P., Ulrich, P., Eds.; NATO ASI Series E, Applied Sciences, 162; Kluver Academic Publishers: Dordrecht, 1989; p 185.
(16) Schwiegk, S.; Vahlenkamp, T.; Xu, Y.; Wegner, G. *Macromolecules* **1992**, *25*, 2513.
(17) Schwiegk, S.; Fischer, H.; Xu, Y.; Kremer, F.; Wegner, G. *Makromol. Chem. Makromol. Symp.* **1991**, *46*, 211.
(18) Wegner, G. *Mol. Cryst. Liq. Cryst.* **1993**, *235*, 1.
(19) Back, R.; Kalvoda, L.; Neher, D.; Ferencz, A.; Wu, J.; Wegner, G. *Chem. Mater.* **1998**, *10*, 2284
(20) Ferencz, A.; Armstrong, N. R.; Wegner, G. *Macromolecules* **1994**, *27*, 1517.
(21) Kalvoda, L.; Back, R.; Ferencz, A.; Neher, D.; Wegner, G. *Mol. Cryst. Liq. Cryst.* **1994**, *252*, 223.
(22) Gattinger, P.; Rengel H.; Neher, D. *Synth. Met.* **1996**, *83*, 245.
(23) Ferencz, A. PhD Thesis, Johannes-Gutenberg-University, Mainz, 1994.
(24) Rengel, H. PhD Thesis, Johannes-Gutenberg-University, Mainz, 1997.
(25) Dekker: C.; Tans, S. J.; Geerligs, L. J.; Bezryadin, A.; Wu, J.; Wegner, G. In *Atomic and Molecular Wires*; Joachim, C., Roth, S., Eds.; Kluwer Academic Publishers: Amsterdam, 1997
(26) Fischer, C. M.; Burghard, M.; Roth, S.; v.Klitzing, K. *Appl. Phys. Lett.* **1995**, *66*, 66.
(27) van de Craats, A. M.; Warman, J. M.; de Haas, M. P.; Adam, D.; Simmerer, J.; Haarer D.; Schuhmacher, P. *Adv. Mater.* **1996**, *8*, 823.
(28) Schouten, P. G.; Warman, J. M.; de Haas, M. P. *J. Phys. Chem.* **1995**, *97*, 9863.
(29) Schouten, P. G. PhD Thesis, Delft University of Technology, 1994 (ISBN 90-73861-22-5).
(30) Schouten, P. G.; Warman, J. M.; de Haas, M. P.; van Nostrum, C. F.; Gelinck, G. H.; Nolte, R. J. M.; Copyn, M. J.; Zwikker, J. W.; Engel, M. K.; Hanack, M.; Chang, Y.; Ford, W. T. *J. Am. Chem. Soc.* **1994**, *116*, 6880.
(31) Warman J. M.; Schouten, P. G. *Appl. Organomet. Chem.* **1996**, *10*, 637.
(32) Schouten, P. G.; Warman, J. M.; Gelinck, G. H.; Copyn, M. J. *J. Phys. Chem.* **1995**, *99*, 11780.
(33) Warman, J. M.; Smit, K. J.; Jonker, S. A.; Verhoeven, J. W.; Oevering, H. Kroon, J.; Paddon-Row: M. N.; Oliver, A. M. *Chem. Phys.* **1993**, *170*, 359.
(34) Closs, G. L.; Miller, J. R. *Science* **1988**, *240*, 440.
(35) Johnson, M. D.; Miller, J. R.; Green N. S.; Closs, G. L. *J. Phys. Chem.* **1989**, *93*, 1173.
(36) Yase, K.; Schwiegk, S.; Lieser, G.; Wegner, G. *Thin Solid Films* **1992**, *210/211*, 22.
(37) Gattinger, P.; Rengel, H.; Back, R.; Neher, D. *J. Phys. Chem. B* **1999**. Manuscript to be submitted for publication.
(38) Ioannidis, A.; Dodelet, J. P. *J. Phys. Chem. B* **1997**, *101*, 901.
(39) Ioannidis, A.; Dodelet, J. P. *J. Phys. Chem. B* **1997**, *101*, 5100.
(40) Harima, Y.; Furusho, S.; Okazaki, K.; Kunugi, Y.; Yamashita, K. *Thin Solid Films* **1997**, *300*, 213.
(41) Bässler, H. *Phys. Status Solod: B* **1993**, *175*, 15.
(42) van de Craats, A. M.; Siebbeles, L. D. A.; Bleyl, I.; Haarer, D.; Berlin, Y. A.; Zharikov, A. A.; Warman, J. M., *J. Phys. Chem. B* **1998**, *102*, 9625.